Real-Time Recognition of Dynamic Hand Postures on a Neuromorphic System

Abstract—To explore the visual processing of the brain, this paper proposes a real-time recognition system of dynamic hand postures on a neuromorphic platform. The hardware system includes a front-end of a Dynamic Video Sensor (DVS) silicon retina and a real-time Spiking Neural Network (SNN) simulator, SpiNNaker, as the back-end. The neural network model is tested both on Matlab and SpiNNaker to validate the transformation from rate-based linear perceptrons to spiking Leaky integrate-and-fire (LIF) neurons. Live recognition with real-time retina input is also carried out to test both the hardware platform and the model. Moreover, different network sizes are configured to evaluate the cost and performance trade-off.

Keywords—spiking neural network (SNN), convolutional neural network (CNN), posture recognition, neuromorphic system.

I. Introduction

PATTERNS or objects in two-dimensional images can be described with four properties [1]: position, geometry (i.e. size, area and shape), colour/texture, and trajectory. Appearance-based methods are the most direct approach to perform pattern recognition where the test image is compared with a set of templates to find the best match for a particular or a combination of properties. However, the 2D projection of an object changes under various illumination, viewing angles, relative positions and distances, making it impossible to represent all appearances of an object in different conditions. To improve reliability, robustness and classification efficiency, approaches such as edge matching [2], divide-and-conquer [3], gradient matching [4], and feature based methods [5], [6] are used. Finding a proper feature for a specific object still remains an open question and there is no process as general, accurate, and energy-efficient as that provided by the brain. It is not a new idea to turn to nature for inspiration. Riesenhuber and Poggio [7], for instance, presented a biologically-inspired model following the organisation of the visual cortex which has the ability to represent relative position- and scale-invariant features. Integrating a rich set of visual features became possible using a feed-forward hierarchical pathway.

To find out how brain recognises objects, we have equipped a biologically-inspired DVS silicon retina [8], which is a good example of low-cost visual processing thanks to its event-driven and redundancy-reducing style of computation; and SpiNNaker system [9], which is a massive parallel computing platform aimed at real-time simulation of SNNs. With the hardware system, we have the ability to explore visual processing by mimicking the functions of various regions along the visual pathway. Building a real-time recognition system of dynamic hand postures is the first step to explore the visual processing in biological way and is a validation of the neuromorphic platform. To match the image properties mentioned above, the retina outputs the position, shape, size and trajectory of the postures. To keep the task simple at first, the postures are of similar size and the goal is to recognise the shape of a hand with moving positions. Tracking the postures with a short memory will be part of the future work.

The dynamic recognition takes the advantage of instinctive temporal processing of SNNs and which are given considerable attention undertaking vision processing. Pattern information can be encoded in the delays between the pre- and post-synaptic spikes since the spiking neurons are capable of computing radial basis functions (RBFs) [10]. Spatio-temporal information can also be stored in the exact firing time rather than the relative delay [11]. Numerous applications using SNN-based vision processing have been successfully carried out. A dual-layer SNN has been trained using Spike Time Dependent Plasticity (STDP) and employed for character recognition [12]. Lee et al. [13] have implemented direction selective filters in real time using spiking neurons, considered as a layer of convolution module in the model of a so called convolutional neural network [14]. Different features, such as Gabor filter features (scale, orientation and frequency) and shape can be modelled as layers of feature maps. Rank order coding, as an alternative to conventional rate-based coding, treats the first spike the most important and has been successfully applied to an orientation detection training process [15]. Deep Belief Networks (DBNs), the 4th generation of artificial neural network, have shown great success in solving classification problems. A recent study [16] has resoundingly mapped an offline-trained DBN onto an efficient event-driven spiking neural network for a digit recognition task.

Section II of this paper presents the details of the hardware of proposed neuromorphic system, including the silicon retina and the SpiNNaker machine. The neural network models were defined and tested on Matlab, and the model structures and experimental results are stated in Section III. In Section IV, the rate-based models are converted into spiking neurons, and real-time live recognition and recorded data experiments are carried out. The contribution of this work is summarised and the future directions are provided in Section V.

II. The Neuromorphic Platform

The outline of the platform is illustrated in Figure 1a, where the hardware system is configured, controlled and monitored by the PC. The jAER [17] event-based processing software on the PC configures the retina and displays the output spikes through a USB link. The host communicates to the SpiNNaker board via Ethernet to set up its runtime parameters and to download the neural network model off-line. It visualises [18] the spiking activity of the network in real-time. The photograph of the hardware platform, Figure 1b, shows that the silicon retina connects to the SpiNNaker 48-node system via a Spartan-6 FPGA board [19].

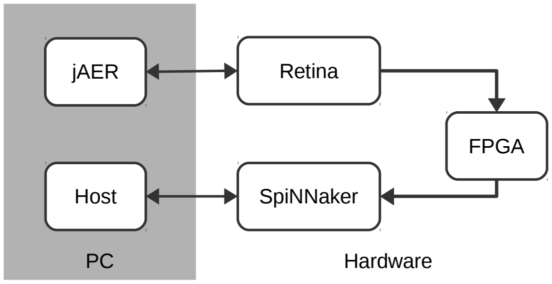

(a) Outline of the platform

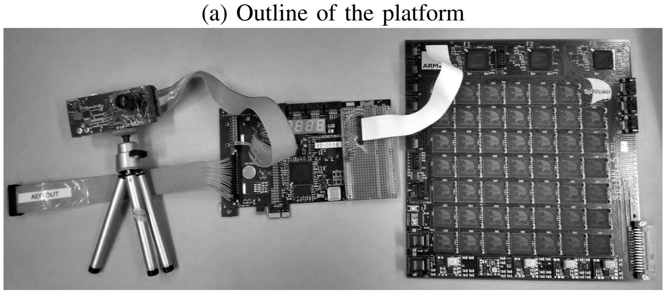

(b) Picture of the hardware platform

Fig. 1: System overview of the dynamic hand posture recognition platform.

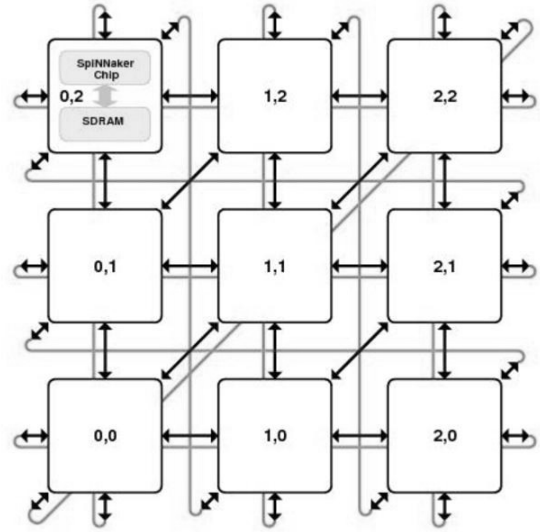

Fig. 2: SpiNNaker system diagram. Each element represents one chip with local memory. Every chip connects to its neighbours through the six bi-directional on-board links.

A. Silicon Retina

The visual input is captured by a DVS silicon retina, which is quite different from conventional video cameras. Each pixel generates spikes when its change in brightness reaches a defined threshold. Thus, instead of buffering video into frames, the activity of pixels is sent out and processed continuously with time. The communication bandwidth is therefore optimised by sending activity only, which is encoded as pixel events using Address-Event Representation (AER [20]) protocol. The level of activity depends on the contrast change; pixels generate spikes faster and more frequently when they are subject to more active change. The sensor is capable of capturing very fast moving objects (e.g., up to 10 K rotations per second), which is equivalent to 100 K conventional frames per second [8].

B. SpiNNaker System

The SpiNNaker project's architecture mimics the human brain's biological structure and functionality. This offers the possibility of utilizing massive parallelism and redundancy, as the brain, to provide resilience in an environment of unreliability and failure of individual components.

In the human brain, communication between its computing elements, or neurons, is achieved by the transmission of electrical 'spikes' along connecting axons. The biological processing of the neuron can be modelled by a digital processor and the axon connectivity can be represented by messages, or information packets, transmitted between a large number of processors which emulate the parallel operation of the billions of neurons comprising the brain.

The engineering of the SpiNNaker concept is illustrated in Figure 2 where the hierarchy of components can be identified. Each element of the toroidal interconnection mesh is a multicore processor known as the 'SpiNNaker Chip' comprising 18 processing cores. Each core is a complete processing subsystem with local memory. It is connected to its local peers via a Network-on-Chip (NoC) which provides high bandwidth onchip communication and to other SpiNNaker chips via links between them. In this way massive parallelism extending to thousands or millions of processors is possible.

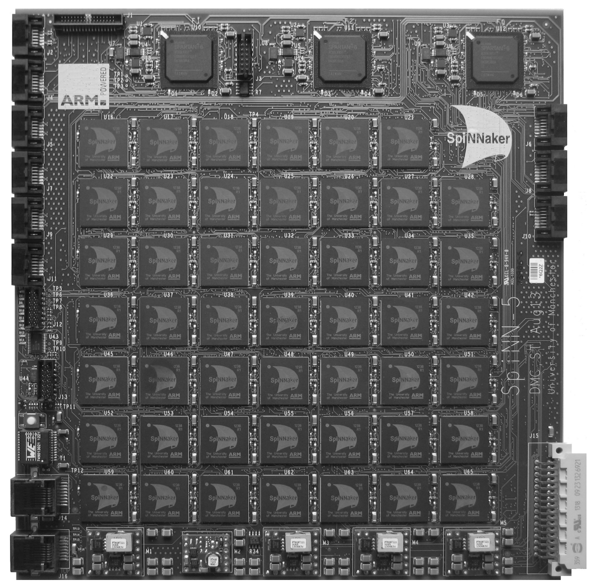

Fig. 3: '103 Machine' PCB

The '103 machine' is the name given to the 48-node board which we use for the hand posture recognition system, see Figure 3. It has 864 ARM processor cores, typically deployed as 768 application, 48 monitor and 48 spare cores. The boards can be connected together to form larger systems using highspeed serial interfaces.

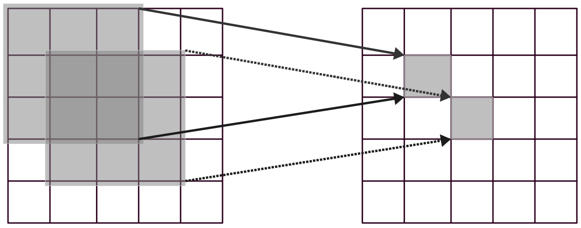

Fig. 4: Each individual neuron in the convolution layer (right matrix) connects to its receptive field using the same kernel. The value of the kernel is represented by the synaptic weights between the connected neurons.

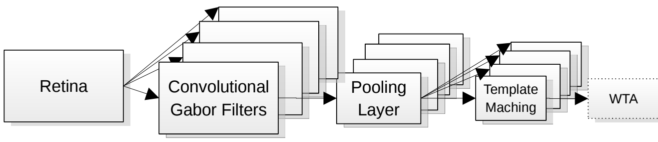

Fig. 5: Model 1. The retina input is convolved with Gabor filters in the second layer, and then shrinks the sizes in the pooling layer. The templates are considered as convolution kernels in the last layer. The WTA circuit can be used as an option to show the template matching result more clearly.

C. Interfacing AER Sensors

Spikes from the silicon retina are injected directly into SpiNNaker via a SPARTAN-6 FPGA board that translates them into a SpiNNaker compatible AER format [21].

From a neural modelling point of view, interfacing the silicon retina is performed using pyNN [22]. The retina is configured as a spike source population that resides on a virtual SpiNNaker chip, to which an AER sensor's spikes are directed, thus abstracting away the hardware details from the user[19]. Besides the retina, we have successfully connected an AER based silicon cochlea [23] to SpiNNaker for a sound localisation task [24].

III. Convolutional Neural Networks

The convolutional neural network (CNN) is well-known as an example of a biologically-inspired model. Figure 4 shows a typical convolutional connection between two layers of neurons. The repeated convolutional kernels are overlapped in the receptive fields of the input neurons.

A. Model Description

There are two CNNs proposed to accomplish the dynamic hand posture recognition task. A straight forward method of template matching was employed at first, followed by a network of multi-layer perceptrons (MLP) trained to improve the recognition performance.

Model 1: Template Matching. Shown in Figure 5 the first layer is the retina input, followed by the convolutional layer, where the kernels are Gabor filters responding to edges of four orientations. The third layer is the pooling layer where the size of the populations shrinks. This down-sampling enables robust classification due to its tolerance to variations in the precise shape of the input. The fourth layer is another convolution layer where the output from the pooling layer is convolved with the templates. The optional layer of Winner-Take-All (WTA) neurons enables a clearer classification result due to the inhibition between the neurons. In the Matlab simulation, the retina input spikes are buffered into 30 ms frames, and the neurons are simple linear perceptrons. The templates were chosen by sampling the output of the pooling layer when given some reference stimulus, see Figure 6.

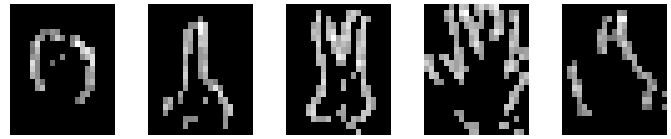

Fig. 6: Templates of the five postures: 'Fist','Index Finger', 'Victory Sign', 'Full Hand' and 'Thumb up'.

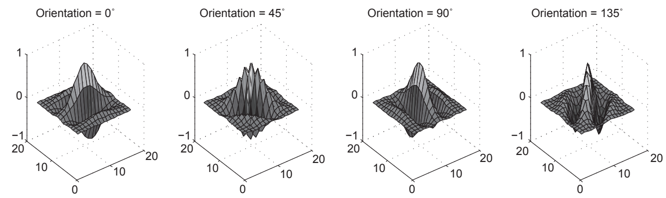

Fig. 7: Real parts of the Gabor filters orienting four directions.

The Gabor filter is well-known as a linear filter for edge detection in image processing. A Gabor filter is a 2D convolution of a Gaussian kernel function and a sinusoidal plane wave; see Equation 1.

$$\begin{aligned} \text{RealParts} &= \exp\left(\frac{-x'^2+y'^2}{2\sigma^2}\right)\cos\left(2\pi\frac{x'}{\lambda}\right) \\ \text{ImaginaryParts} &= \exp\left(\frac{-x'^2+y'^2}{2\sigma^2}\right)\sin\left(2\pi\frac{x'}{\lambda}\right) \\ \text{where} &: \\ x' &= x\cos(\theta)+y\sin(\theta) \\ y' &= -x\sin(\theta)+y\cos(\theta) \end{aligned} \tag{1}$$

θ represents the orientation of the filter, λ is the wavelength of the sine wave, and σ is the standard deviation of the Gaussian envelope. The frequency and orientation features are similar to the responses of V1 neurons in the human visual system. Only the real parts of the Gabor filters (see Figure 7) are used as the convolutional kernels to configure the weights between the input layer and the Gabor filter layer.

The output score of a convolution is determined by the matching degree between the input and the kernel. Regarding the template matching layer, each neuron in a population responds to how closely its receptive field matches the specific template. The position of moving gesture is also naturally encoded in the address of template matching neuron. Thus, there are five populations of template matching neurons, one for each hand posture listed.

Model 2: Trained MLP. Inspired by the research of Lecun [25], we designed a combined network model with MLP

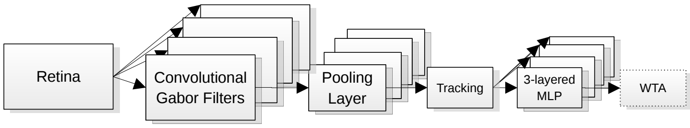

Fig. 8: Model 2. The retina input convolves with Gabor filters in the second layer, and then shrinks the sizes in the pooling layer. The following tracking layer finds the most active area of some fixed size, moves the posture to the centre and pushes the image to the trained MLP. The winner-take-all (WTA) layer can be used as an option to show the template matching result more clearly.

and CNN (Figure 8). The first three layers are exactly the as the previous model. The training images for the 3-layered MLP are of same size and the posture is centred in the images. Therefore, a tracking layer plays an important role to find the most active region and forward the centred image to the next layer.

B. Experimental Set-up

In order to evaluate the cost and performance trade-offs in optimizing the number of neural components, both the convolutional models described above were tested at different scales. Five videos of every posture were captured from the silicon retina in AER format, all of similar size and moving clock-wise in front of the retina. The videos are cut into frames (30 ms per frame) and presented to the convolutional networks. The configurations of the networks are listed in Table I. The integration layer is not necessary in a convolutional network, but is used here to decrease the number of synaptic connections.

C. Experimental Results

In Figure 9 the first two plots refer to Model 1, using template matching. Each colour represents one of the recognition populations. Each point in the plot is the highest neuronal response in the recognition population during the time of one frame (30 ms). The neuronal response, 'the spiking rate', is normalised to [-1, 1]. It can be seen that the higher resolution input makes the boundaries between the classes clearer. On the other hand, recognition only happens when the test image and template are similar enough. The templates are only selected from the frames where the gestures are moving towards the right, and the gestures are moving clockwise in the videos, thus, all the peaks in plot 1 correspond with moments when the gesture moves towards right. It is notable that the higher resolution causes the recogniser to be more sensitive to the differences between the test data and the template, while the smaller neural network can recognize more generalized patterns. Therefore, a threshold is required to differentiate between data that is close enough and that which is not. Since the gestures are moving in four different directions during the clockwise movement, a rejection rate (i.e. none of the template is matched) of 75% is to be expected.

The latter two plots of Figure 9 refer to Model 2. The three-layer MLP network significantly improves the recognition rate

TABLE I: Sizes of the convolutional neural networks.

(a) Model 1: Template matching

	Full Resolution 128 × 128		**Sub-sampled Resolution 32 × 32**	
	Population Size	Connections per Neuron	Population Size	Connections per Neuron
Retinal Input	128 × 128	1	32 × 32	4 × 4
Gabor Filter	112×112×4	17 × 17	28×28×4	5 × 5
Pooling Layer	36×36×4	5 × 5	null	null
Integration Layer	36 × 36	4	28 × 28	4
Template Matching	16×16×5	21 × 21	14×14×5	15 × 15
Total	74,320	15,216,512	5,925	318,420

(b) Model 2: Trained MLP

	Full Resolution 128 × 128		**Sub-sampled Resolution 32 × 32**	
	Population Size	Connections per Neuron	Population Size	Connections per Neuron
Tracked Input	21 × 21	null	15 × 15	null
Hidden Layer	10	21×21×10	10	15×15×10
Recognition Layer	5	5×10	5	5×10
Total	456	4,460	240	2,300

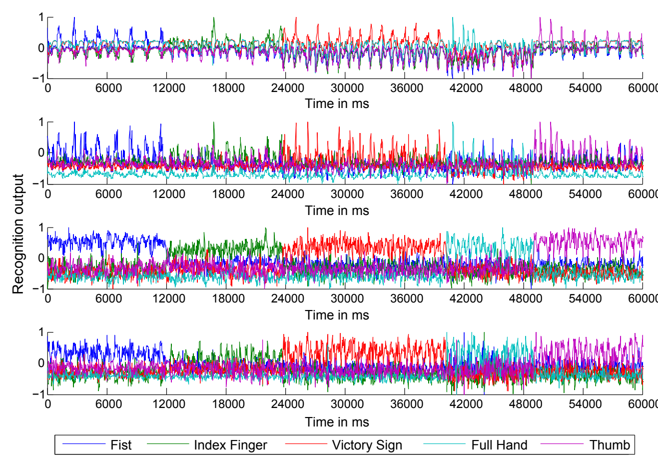

Fig. 9: Neural responses with time of four experiments to the same recorded moving postures. The recognition output is normalised to [-1, 1]. Every point represents the highest response in a specific population (different colour) for a 30 ms frame. The 1st plot refers to Model 1 with the full input resolution, and the 2nd plot Model 1 with the sub-sampled input resolution; and the 3rd and fourth plots both refer to Model 2, and with high and low input resolution respectively.

TABLE II: Recognition results in %

		Model 1		Model 2	
		High Resolution	Low Resolution	High Resolution	Low Resolution
Fist	Correct	99.11	99.23	96.24	84.21
(399 Frames)	Reject	71.93	67.42	Null	Null
Index Finger	Correct	92.98	80.00	94.39	71.69
(392 Frames)	Reject	70.92	75.77	Null	Null
Victory Sign	Correct	96.56	93.07	95.64	87.66
(551 Frames)	Reject	73.68	81.67	Null	Null
Full Hand	Correct	95.65	72.41	93.52	72.01
(293 Frames)	Reject	92.15	90.10	Null	Null
Thumb up	Correct	89.61	84.44	96.68	74.68
(391 Frames)	Reject	80.31	76.98	Null	Null
Average	Correct	89.61	84.44	96.68	74.68
(391 Frames)	Reject	80.31	76.98	Null	Null

and can generalise the pattern. There is no rejection rate for Model 2, since the MLP is trained with all the moving directions of the postures.

Detailed results are listed in Table II. The correct recognition rate is calculated from the non-rejected frames. The lower resolution of the 32×32 retina input is adequate for this gesture recognition task. The smaller network uses only 1/10th the number of neurons and 1/50th the number of synaptic connections compared with the full resolution network, while the recognition rate drops only around by 10% with Model 1 and 15% with Model 2.

IV. Real-Time Recognition on SpiNNaker

A. Moving from Rate-based Artificial Neurons to Spiking Neurons

It remains a challenge to transform traditional artificial neural networks into spiking ones. There are attempts [26] [27] to estimate the output firing rate of the LIF neurons (Equation 2) under certain conditions.

$$\frac{\mathrm{d}V(t)}{\mathrm{d}t} = -\frac{V(t) - V_{rest}}{\tau_m} + \frac{I(t)}{C_m} \tag{2}$$

The membrane potential V changes in response to input current I, starting at the resting membrane potential V_{rest}, where the membrane time constant is $\tau_m = R_m C_m$, R_m is the membrane resistance and C_m is the membrane capacitance.

Given a constant current injection I, the response function, i.e. firing rate, of the LIF neuron is

$$\lambda_{out} = \left[t_{ref} - \tau_m \ln \left(1 - \frac{V_{th} - V_{rest}}{IR_m} \right) \right]^{-1} \tag{3}$$

when $IR_m > V_{th} - V_{rest}$, otherwise the membrane potential cannot reach the threshold V_{th} and the output firing rate is zero. The absolute refractory period t_{ref} is included, where all input during this period is invalid. In a more realistic scenario, the post-synaptic potentials (PSPs) are triggered by the spikes generated from the neuron's pre-synaptic neurons other than a constant current. Assume that the synaptic inputs are Poisson spike trains, the membrane potential of the LIF neuron is considered as a diffusion process. Equation 2 can be modelled as a stochastic differential equation referring to Ornstein-Uhlenbeck process,

$$\tau_m \frac{\mathrm{d}V(t)}{\mathrm{d}t} = -[V(t) - V_{rest}] + \mu + \sigma\sqrt{2\tau_m}\xi(t) \tag{4}$$

where

$$\begin{aligned} \mu &= \tau_m(\mathbf{w_E} \cdot \lambda_\mathbf{E} - \mathbf{w_I} \cdot \lambda_\mathbf{I}) \\ \sigma^2 &= \tfrac{\tau_m}{2}\left(\mathbf{w_E^2} \cdot \lambda_\mathbf{E} + \mathbf{w_I^2} \cdot \lambda_\mathbf{I}\right) \end{aligned} \tag{5}$$

are the conditional mean and variance of the membrane potential. The delta-correlated process $\xi(t)$ is Gaussian white noise with zero mean, $\mathbf{w_E}$ and $\mathbf{w_I}$ stand for the weight vectors of the excitatory and the inhibitory synapses, and λ represents the vector of the input firing rate. The response function of the LIF neuron with Poisson input spike trains is given by the Siegert function [28],

$$\begin{aligned} \lambda_{out} = \Bigg(\tau_{ref} + \frac{\tau_Q}{\sigma_Q}\sqrt{\frac{\pi}{2}} \int_{V_{rest}}^{V_{th}} \mathrm{d}u \exp\left(\frac{u - \mu_Q}{\sqrt{2}\sigma_Q}\right)^2 \\ \cdot \left[1 + \mathrm{erf}\left(\frac{u - \mu_Q}{\sqrt{2}\sigma_Q}\right)\right]\Bigg)^{-1} \end{aligned} \tag{6}$$

where τ_Q, μ_Q, σ_Q are identical to τ_m, μ, σ in Equation 5, and erf is the error function.

Still there are some limitations on the response function. For the diffusion process, only small amplitude (weight) of the PostSynaptic Potentials (PSPs) generated by a large amount of input spikes (high spiking rate) work under this circumstance; plus, the delta function is required, i.e. the synaptic time constant is considered to be zero. Thus only a rough approximation of the output spike rate has been determined. Secondly, given the input spike rates of the pre-synaptic neurons, the parameters of the LIF neuron and the output spiking rate, how to tune every corresponding synaptic weight remains a difficult task.

B. Live Recognition

We implemented the prototype of the dynamic posture recognition system on SpiNNaker using LIF neurons. The input retina layer consists of 128×128 neurons; each Gabor filter has 112×112 valid neurons, since the kernel size is 17×17; each pooling layer is as big as 36×36, convolving with five template kernels (21×21); thus, the recognition populations are 16×16 neurons each. Altogether 74,320 neurons and 15,216,512 synapses, use up to 19 chips (290 cores) on a 48-node board, see Table Ia. Regarding the lower resolution of 32×32 retinal input, (Table Ib) consists of 5,925 neurons and 318,420 synapses taking up only two chips (31 cores) of the board.

Figure 10 shows snapshots of neural responses of some populations during real-time recognition. Figure 10a is a snapshot of the Gabor population which prefers the horizontal direction, given the input posture of a 'Fist'; and Figure 10b shows the activity of the neurons in the integration layer, given a 'Victory Sign'. And the active neurons in the visualiser in Figure 10c are pointing out the position of the recognised pattern the 'Index finger'. All the supporting demonstrative videos can be found on YouTube [29], [30], [31].

(a) Neural responses of the Gabor filter layer orienting to the horizontal direction [29]

(b) Neural responses of the integrate layer [30]

(c) Snapshot of the neuron responses of the template matching layer [31]

Fig. 10: Snapshots of the real-time dynamic posture recognition system on SpiNNaker.

C. Recognition of Recorded Data

To compare with the results of the experiments carried out with Matlab (in Section III-C), the same recorded retinal data is conducted into SpiNNaker. The recorded data is presented as spike source array in the system with 128×128 input (see Figure 12a) while the data is forwarded to a sub-sampling layer of 32×32 resolution in the system of the smaller network (see Figure 13a). The output spikes generated from the recognition populations with time are shown in Figures 12 and 13 for full resolution and lower systems respectively. More spikes are generated during the period when the preferred input posture is shown.

Correspondingly, the spiking rates of each recognition population is sampled into frames (Figure 11) to make a comparison with the Matlab simulation. Each colour represents one recognition population, and the spike activity goes higher when the input posture matches the template. Firstly, the spike rates are sampled into 30 ms frames which is in accordance with the Matlab experiments. In the Matlab simulation, the templates are trained with cut frames and so the test images are also fixed to the same length frames. Otherwise, the recogniser will

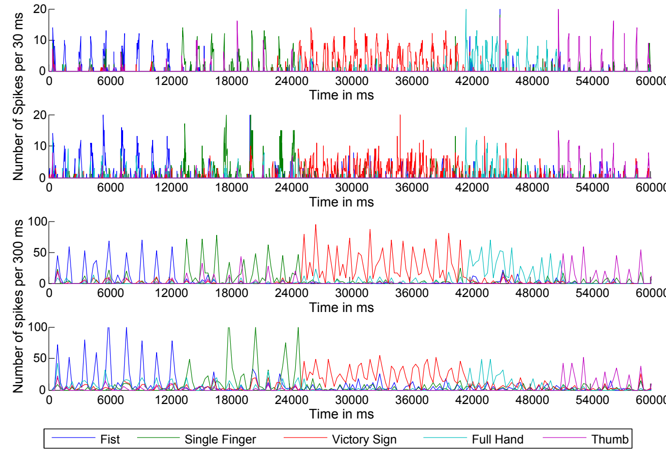

Fig. 11: Real-time neural responses of two experiments on SpiNNaker with time to the same recorded postures. These two experiments only differ in input resolution. The result of the high input resolution test is plotted the first with a sample frame of 30 ms; while the 3rd plot shows the same result with a sample frame of 300 ms. The other two plots refer to the smaller input resolution. Every point represents the over all number of spikes of a specific population (different colour) in a 'frame'.

not work properly because of the replications of the moving posture. Contrasting this, the spiking rates can be sampled to various frame lengths. Thus, the other two plots in the figure illustrate the classification in a wider window of 300 ms. From Table III, the recognition and rejection rates are quantified as percentages.

Comparing with the results of Matlab simulation (Table II), the recognition rate is about 10% lower both in high and low resolution, and the rejection rate increases by around 10%. However, by changing the frame length to 300 ms both of recognition rates reach or exceed the Matlab simulation, meanwhile the rejection rate dropped dramatically. It is in accordance with the natural visual responses, which means, the longer an object shows the more accurate the recognition will be. In terms of the performance, between the two scales there is a smaller gap of the recognition rates as the window length grows. The correct recognitions of three postures out of five are over 90% using the smaller network. Considering the cost and performance trade-off, with only 1/10th resources required, the performance of the small network is acceptable and can be even improved after applying tracking and learning. Regarding the latency between the retinal input and the recognition, we compared the spiking peak of the Matlab simulation and the real-time SpiNNaker test. The overall latency is about 1150 ms from a posture being shown to its recognition.

V. Conclusion and Future Work

In this paper, we implement a dynamic hand posture recognition system completely running on a hardware neuromorphic platform. The network model is translated from linear perceptrons to LIF spiking neurons with 10% drop of accuracy in 30 ms windowing; while the performance reach and even

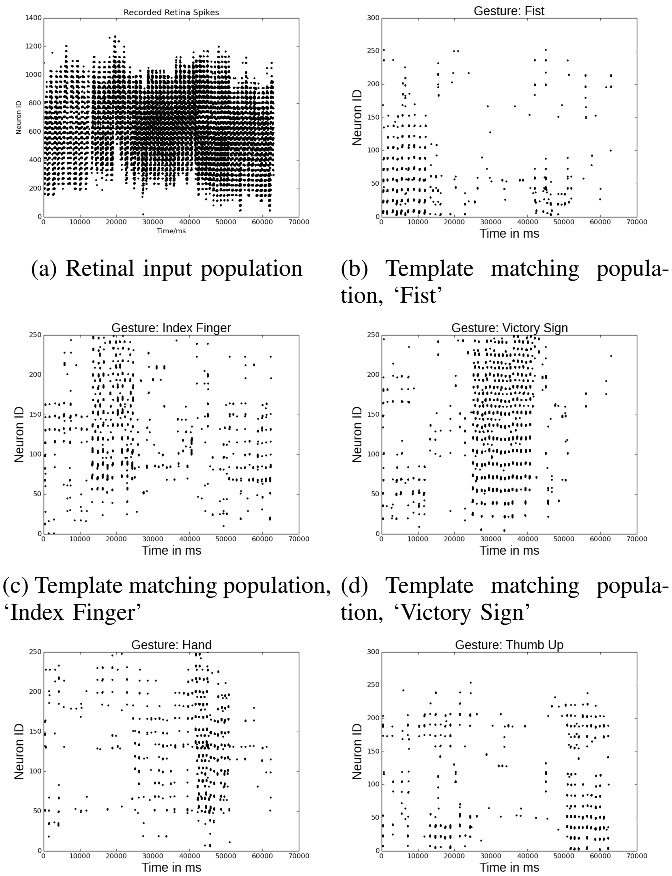

(a) Retinal input population
(b) Template matching population, 'Fist'
(c) Template matching population, 'Index Finger'
(d) Template matching population, 'Victory Sign'
(e) Template matching population, 'Full Hand'
(f) Template matching population, 'Thumb Up'

Fig. 12: Spikes captured during the live recognition of the recorded retinal input with the resolution of 128×128.

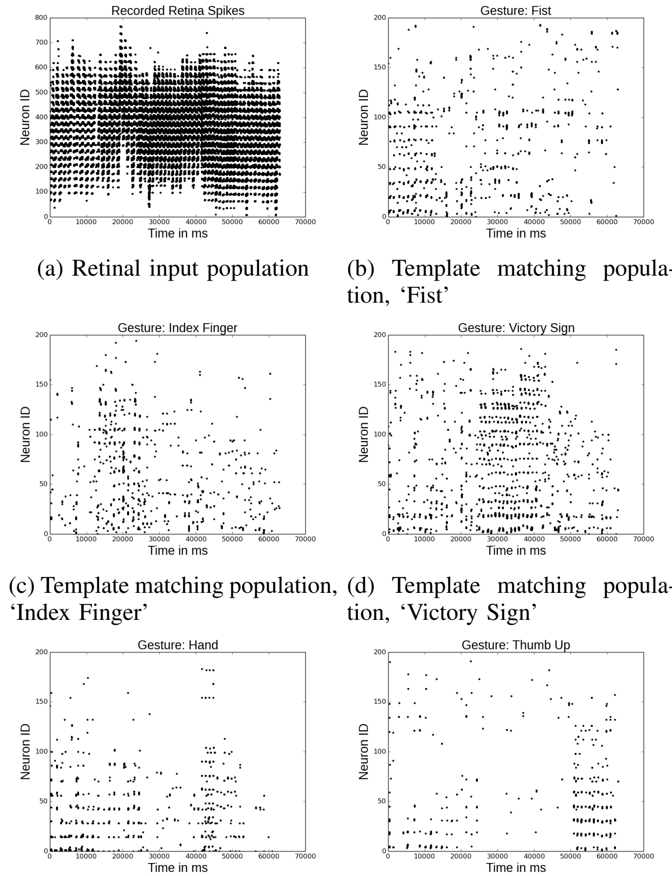

(a) Retinal input population
(b) Template matching population, 'Fist'
(c) Template matching population, 'Index Finger'
(d) Template matching population, 'Victory Sign'
(e) Template matching population, 'Full Hand'
(f) Template matching population, 'Thumb Up'

Fig. 13: Spikes captured during the live recognition of the recorded retinal input with the resolution of 32×32.

TABLE III: Real-time recognition results on SpiNNaker in %

		30 ms per frame		**300 ms per frame**	
		High Resolution	Low Resolution	High Resolution	Low Resolution
Fist	Correct	91.78	78.02	100	92.31
	Reject	82.78	78.54	70.73	68.29
Index Finger	Correct	78.25	78.25	88.24	72.22
	Reject	80.46	73.56	57.50	55.00
Victory Sign	Correct	96.48	86.27	95.00	92.50
	Reject	64.46	72.68	28.57	28.57
Full Hand	Correct	85.29	60.78	90.00	75.00
	Reject	67.31	83.65	35.48	61.29
Thumb up	Correct	84.09	88.10	91.67	100
	Reject	87.54	73.81	66.67	66.67

exceed the Matlab version when the window length is set to 300 ms. Different network sizes are configured to the cost and performance trade-off. In the test of Matlab simulation, the recognition rate of the smaller network is 10% lower for the template matching model and 15% lower for the trained MLP model. For the real-time experiments, both the bigger network of $74,320$ LIF neurons and $15,216,512$ synapses and the smaller (1/10 of the neurons and 1/50 of the synapses) run smoothly on SpiNNaker with a overall delay of 1150 ms.

The future work on this topic will include further collaboration with biologists and neuroscientist of vision systems, especially concentrating on the orientation detection region. To equip the system with tracking is another importance where the recognition performance will be increased and the short-term memory of a gesture route can be stored. Using the idea of HMMs [32] to spiking neural networks may be a good approach.

VI. Acknowledgement

This research was supported by Samsung under their GRO programme. The authors appreciate the collaboration with Prof. Bernabé Linares-Barranco and Luis Camunas-Mesa on the silicon retina. The authors would also like to thank the meaningful discussions with Evangelos Stromatias, Patrick Camilleri and Michael Hopkins. And Johnathon Heathcote as well as Cameron Patterson are thanked for their final proofreading of the paper.

References

[1] S. G. Wysoski, L. Benuskova, and N. Kasabov, "Fast and adaptive network of spiking neurons for multi-view visual pattern recognition," *Neurocomputing*, vol. 71, no. 13, pp. 2563–2575, 2008.

[2] J. Canny, "A computational approach to edge detection," *Pattern Analysis and Machine Intelligence, IEEE Transactions on*, no. 6, pp. 679–698, 1986.

[3] Ö. Toygar and A. Acan, "Multiple classifier implementation of a divide-and-conquer approach using appearance-based statistical methods for face recognition," *Pattern Recognition Letters*, vol. 25, no. 12, pp. 1421–1430, 2004.

[4] S.-D. Wei and S.-H. Lai, "Robust and efficient image alignment based on relative gradient matching," *Image Processing, IEEE Transactions on*, vol. 15, no. 10, pp. 2936–2943, 2006.

[5] D. G. Lowe, "Distinctive image features from scale-invariant keypoints," *International journal of computer vision*, vol. 60, no. 2, pp. 91–110, 2004.

[6] H. Bay, A. Ess, T. Tuytelaars, and L. Van Gool, "Speeded-up robust features (SURF)," *Computer vision and image understanding*, vol. 110, no. 3, pp. 346–359, 2008.

[7] M. Riesenhuber and T. Poggio, "Hierarchical models of object recognition in cortex," *Nature neuroscience*, vol. 2, no. 11, pp. 1019–1025, 1999.

[8] J. A. Leñero-Bardallo, T. Serrano-Gotarredona, and B. Linares-Barranco, "A 3.6 s latency asynchronous frame-free event-driven dynamic-vision-sensor," *Solid-State Circuits, IEEE Journal of*, vol. 46, no. 6, pp. 1443–1455, 2011.

[9] S. B. Furber, F. Galluppi, S. Temple, and L. A. Plana, "The SpiNNaker Project," 2014.

[10] J. J. Hopfield, "Pattern recognition computation using action potential timing for stimulus representation," *Nature*, vol. 376, no. 6535, pp. 33–36, 1995.

[11] T. Natschläger and B. Ruf, "Spatial and temporal pattern analysis via spiking neurons," *Network: Computation in Neural Systems*, vol. 9, no. 3, pp. 319–332, 1998.

[12] A. Gupta and L. N. Long, "Character recognition using spiking neural networks," in *Neural Networks, 2007. IJCNN 2007. International Joint Conference on*, pp. 53–58, IEEE, 2007.

[13] J. H. Lee, P. Park, C.-W. Shin, H. Ryu, B. C. Kang, and T. Delbruck, "Touchless hand gesture UI with instantaneous responses," in *Image Processing (ICIP), 2012 19th IEEE International Conference on*, pp. 1957–1960, Sept 2012.

[14] L. Camunas-Mesa, C. Zamarreno-Ramos, A. Linares-Barranco, A. J. Acosta-Jimenez, T. Serrano-Gotarredona, and B. Linares-Barranco, "An event-driven multi-kernel convolution processor module for event-driven vision sensors," *Solid-State Circuits, IEEE Journal of*, vol. 47, no. 2, pp. 504–517, 2012.

[15] A. Delorme, L. Perrinet, and S. J. Thorpe, "Networks of integrate-and-fire neurons using rank order coding b: spike timing dependent plasticity and emergence of orientation selectivity," *Neurocomputing*, vol. 38, pp. 539–545, 2001.

[16] P. O'Connor, D. Neil, S.-C. Liu, T. Delbruck, and M. Pfeiffer, "Real-time classification and sensor fusion with a spiking deep belief network," *Frontiers in neuroscience*, vol. 7, 2013.

[17] T. Delbruck, "Frame-free dynamic digital vision," in *Proceedings of Intl. Symp. on Secure-Life Electronics, Advanced Electronics for Quality Life and Society*, pp. 21–26, 2008.

[18] C. Patterson, F. Galluppi, A. Rast, and S. Furber, "Visualising large-scale neural network models in real-time," in *Neural Networks (IJCNN), The 2012 International Joint Conference on*, pp. 1–8, 2012.

[19] F. Galluppi, K. Brohan, S. Davidson, T. Serrano-Gotarredona, J.-A. P. Carrasco, B. Linares-Barranco, and S. Furber, "A real-time, event-driven neuromorphic system for goal-directed attentional selection," in *Neural Information Processing*, pp. 226–233, Springer, 2012.

[20] J. Lazzaro and J. Wawrzynek, "A multi-sender asynchronous extension to the aer protocol," in *Advanced Research in VLSI, Conference on*, pp. 158–158, IEEE Computer Society, 1995.

[21] L. A. Plana, "AppNote 8 - Interfacing AER devices to SpiNNaker using an FPGA." https://spinnaker.cs.man.ac.uk/tiki-download_wiki_attachment.php?attId=20, 4 2013.

[22] A. P. Davison, D. Brüderle, J. Eppler, J. Kremkow, E. Muller, D. Pecevski, L. Perrinet, and P. Yger, "Pynn: a common interface for neuronal network simulators," *Frontiers in neuroinformatics*, vol. 2, 2008.

[23] S.-C. Liu, A. van Schaik, B. Minch, and T. Delbruck, "Event-based 64-channel binaural silicon cochlea with q enhancement mechanisms," in *Circuits and Systems (ISCAS), Proceedings of 2010 IEEE International Symposium on*, pp. 2027–2030, May 2010.

[24] Q. Liu, C. Patterson, S. Furber, Z. Huang, Y. Hou, and H. Zhang, "Modeling populations of spiking neurons for fine timing sound localization," in *Neural Networks (IJCNN), The 2013 International Joint Conference on*, pp. 1–8, Aug 2013.

[25] Y. LeCun, L. Bottou, Y. Bengio, and P. Haffner, "Gradient-based learning applied to document recognition," *Proceedings of the IEEE*, vol. 86, no. 11, pp. 2278–2324, 1998.

[26] G. La Camera, M. Giugliano, W. Senn, and S. Fusi, "The response of cortical neurons to in vivo-like input current: theory and experiment," *Biological cybernetics*, vol. 99, no. 4-5, pp. 279–301, 2008.

[27] A. N. Burkitt, "A review of the integrate-and-fire neuron model: I. homogeneous synaptic input," *Biological cybernetics*, vol. 95, no. 1, pp. 1–19, 2006.

[28] A. J. Siegert, "On the first passage time probability problem," *Physical Review*, vol. 81, no. 4, p. 617, 1951.

[29] Q. Liu, "A gabor filter prefers the horizontal lines running on SpiNNaker in real-time ." https://www.youtube.com/watch?v=PvJy6RKAJhw&feature=youtu.be&list=PLxZ1W-Upr3eoQuLxq87qpUL-CwSphtEBJ, Sept. 2014.

[30] Q. Liu, "Feature extraction of live retinal input." http://youtu.be/FZJshPCJ1pg?list=PLxZ1W-Upr3eoQuLxq87qpUL-CwSphtEBJ, Sept. 2014.

[31] Q. Liu, "Live dynamic posture recognition on SpiNNaker." http://youtu.be/yxN90aGGKvg?list=PLxZ1W-Upr3eoQuLxq87qpUL-CwSphtEBJ, Sept. 2014.

[32] M. Elmezain, A. Al-Hamadi, J. Appenrodt, and B. Michaelis, "A hidden markov model-based isolated and meaningful hand gesture recognition," *International Journal of Electrical, Computer, and Systems Engineering*, vol. 3, no. 3, pp. 156–163, 2009.